Received: 14 September 2018 | Revised: 13 August 2019 | Accepted: 28 October 2019

DOI: 10.1002/rnc.4826

RESEARCH ARTICLE

WILEY

Robust output tracking of constrained perturbed linear systems via model predictive sliding mode control

M. Steinberger[1] | **I. Castillo**[1] | **M. Horn**[1] | **L. Fridman**[2]

[1]Institute of Automation and Control, Graz University of Technology, Graz, Austria

[2]Facultad de Ingeniería, Universidad Nacional Autónoma de México (UNAM), México City, México

Correspondence
M. Steinberger, Institute of Automation and Control, Graz University of Technology, Inffeldgasse 21b, 8010 Graz, Austria.
Email: martin.steinberger@tugraz.at

Funding information
Christian Doppler Research Association; Austrian Federal Ministry for Digital and Economic Affairs; National Foundation for Research, Technology and Development; CONACYT (Consejo Nacional de Ciencia y Tecnologia), Grant/Award Number: 282013; PAPIIT-UNAM (Programa de Apoyo a Proyectos de Investigación e Innovación Tecnológica), Grant/Award Number: IN 115419; H2020 Marie Skłodowska-Curie Actions, Grant/Award Number: 734832

Summary

A robustifying strategy for constrained linear multivariable systems is proposed. A combination of tracking model predictive control with output integral sliding mode techniques is used to completely reject bounded matched perturbations. It can be guaranteed that all constraints on inputs, states, and outputs are satisfied although only output information is used. Finally, real-world experiments with an unstable plant are presented in order to demonstrate the validity and the effectiveness of the proposed approach.

KEYWORDS

linear model predictive control, output integral sliding mode, output tracking, sliding mode control

1 | INTRODUCTION

Model predictive control (MPC) has become one of the most widely used control techniques due to its capability to explicitly handle constraints in the controller.[1-4] One of the important milestones is the paper of Mayne et al[5] that forms the basis for theoretical analysis in terms of stability and optimality. It is shown that terminal costs and terminal sets are the main ingredients to ensure stability for a huge number of different MPC formulations.

There are also extensions of MPC to track piecewise constant reference signals.[6] Generalized conditions for stability are given in the work of Mayne and Falugi[7] to increase the region of attraction for tracking equilibrium states. Further extensions deal with the robustness with respect to external disturbances and parameter variations. They come in very different flavors (see, eg, the work of Mayne[8] for an overview). The price to be paid for robust MPC formulations is an increasing complexity of the underlying optimization problems with the respective computational cost.

With regard to robustness, sliding mode control (SMC) is one of the most promising techniques that has been developed over many decades.[9-11] Especially, the ability to completely reject matched bounded perturbations is one of its main distinctive features. It comes together with the advantage of a low number of control parameters and simple implementation. The drawback of SMC is that constraint handling in general is nontrivial.

In the recent years, one line of research is to combine ideas from generalized predictive control[3] with SMC. In a paper by Garcia-Gabin et al,[12] a sliding variable is predicted for a SISO system modeled by its transfer function. This prediction is incorporated into the performance index of an optimization problem. The use of additional constraints guarantees that the sliding variable decreases asymptotically to zero. A first-order SISO system with constant delay is considered in the work of Perez et al.[13] In this work, additional conditions are imposed in the optimization problem to ensure discrete-time quasi-sliding with respect to a predicted sliding variable. Recently, first steps toward nonlinear generalized predictive control with SMC are published by Errouissi et al.[14] However, constraints are not taken into account.

A second line in literature uses the concept of integral SMC[9,15] (ISMC) to combine ideas from MPC with SMC. Rubagotti et al[16] propose a combination of discrete-time robust MPC with continuous time ISM to stabilize the origin under the presence of matched and unmatched perturbations. In the work of Raimondo et al,[17] a multirate sliding mode disturbance compensation for MPC is shown. It makes use of the properties of discrete-time SMC[18] to force the sliding variable to zero in one sampling step. Tightened MPC is used in the outer loop to handle unmatched perturbations. Both papers aim to stabilize the origin.

In contrast, the authors of this paper proposed first steps toward a scheme combining the strengths of SMC and MPC using output information only.[19] It exploits the properties of an output integral sliding mode observer (OISMO) and output integral sliding mode controller[20,21] (OISMC). Compared to this conference paper,[19] this article features the following main contributions:

(a) A detailed scheme consisting of an inner and outer loop is proposed to ensure complete elimination of matched perturbations without violating the given constraints and using output information only.
(b) The MPC formulation in the outer loop is extended and the stability of the overall feedback loops is proven.
(c) An unstable mechanical system is used to show the properties of the proposed method in a real-world application. Additionally, the effect of different sampling times that are used for discrete-time realizations of the inner loop are investigated with respect to the ideal sliding mode behavior.

The remainder of this paper is structured as follows: In Section 2, the problem to be tackled is formulated. After that, the proposed approach "model predictive sliding" (MPS) consisting of an OISMO, OISMC, and a tracking MPC is described in detail in Section 3. In Section 4, the properties of the method are exemplified using simulations as well as measurements on a lab experiment. Finally, conclusions are drawn and further extensions are discussed in Section 5.

2 | PROBLEM STATEMENT

Consider a linear time-invariant multivariable system

$$\dot{x}(t) = Ax(t) + B\left(u(t) + w(t)\right) \tag{1a}$$

$$y(t) = Cx(t), \tag{1b}$$

with state vector $x(t) \in \mathbb{R}^n$, inputs $u(t) \in \mathbb{R}^m$, and outputs $y(t) \in \mathbb{R}^p$ that is subject to perturbations $w(t) \in \mathbb{R}^m$. Matrices A, B, and C are constant, of proper dimensions and known. The following assumptions are imposed on system (1):

Assumption 1 (Properties of plant, perturbation and constraints)**.**

(a) Input and output matrices have full rank, ie, rank $B = m$ and rank $C = p$. The pair (A, B) is controllable, the pair (A, C) is observable.
(b) The initial states are unknown but bounded, ie, $\|x(0)\| \leq \mu$.
(c) The perturbations are unknown but bounded in magnitude such that $\|w(t)\| \leq w_{\max}$.
(d) The dimensions of disturbances, outputs, and states fulfill $m < p < n$.
(e) The system is of relative degree one, ie, rank$(CB) = m$.
(f) The constraints for inputs $u \in \mathbb{U}$, states $x \in \mathbb{X}$, and outputs $y \in \mathbb{Y}$ are compact sets.

The main goal of this work is to design an output tracking controller for system (1) capable of rejecting time-varying bounded perturbations $w(t)$. It has to be ensured that all constraints on inputs, states, and outputs are satisfied and that stability of the closed loop is guaranteed.

3 | MODEL PREDICTIVE SMC

Figure 1 illustrates the structure of the proposed control architecture.[19] It consists of a continuous-time inner loop and a discrete-time outer loop coupled via sample (S) and hold (H) elements.

The plant states are estimated using output integral sliding mode (OISM) techniques in the inner loop. Additionally, a control signal u_O is generated to counteract perturbations. In the outer loop, an output tracking MPC provides a nominal control signal u_M for the system without perturbations. This control signal as well as u_O are bounded in magnitude to make sure that neither constraints for states nor for outputs are violated. Their sum

$$u(t) = u_M(t) + u_O(t) \tag{2}$$

is applied at the plant. Detailed descriptions of the individual parts are given in the next sections.

3.1 | Output ISMC and observation

The OISM block in the inner loop of Figure 1 consists of a Luenberger observer (LO), an OISMO, and an OISMC connected according to Figure 2.

3.1.1 | Output integral sliding mode controller

In the first step, it is assumed that the estimates $\tilde{x}$ for the plant states x are known.[20,21] A sliding variable

$$s(t) = G\left(y(t) - y(0) - \int_0^t \left[CA\tilde{x}(\tau) + CBu_M(\tau)\right] d\tau\right) \tag{3}$$

with $G \in \mathbb{R}^{m\times p}$ is chosen such that $\det(GCB) \neq 0$. It represents the weighted deviation of the actual plant output from the output of the nominal system under nominal control u_M. The so-called unit vector approach[10] is applied to determine the

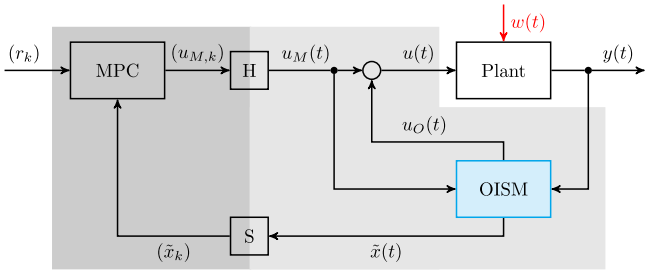

FIGURE 1 Overall structure of the control loop consisting of a constrained plant that is subject to perturbations, a continuous-time controller (light gray) and a discrete-time controller (dark gray). MPC, model predictive control; OISM, output integral sliding mode [Colour figure can be viewed at wileyonlinelibrary.com]

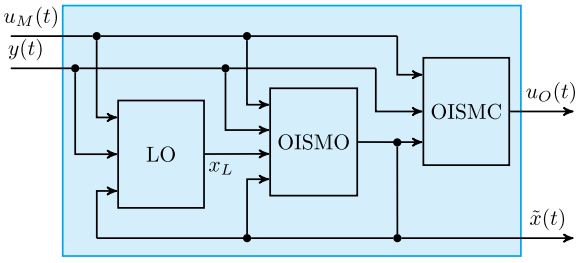

FIGURE 2 Inner structure of the output integral sliding mode (OISM) block from Figure 1 providing a discontinuous control signal u_O and estimated plant states $\tilde{x}$. LO, Luenberger observer; OISMC, OISM controller; OISMO, OISM observer [Colour figure can be viewed at wileyonlinelibrary.com]

control signal of the inner loop in Figure 1, resulting in

$$u_O(t) = -\beta(t)(GCB)^{-1}\frac{s(t)}{\|s(t)\|}. \tag{4}$$

Sliding mode is enforced for sufficiently large $\beta(t) \in \mathbb{R}$ where all solutions of the closed-loop system are understood in the sense of Filippov.[22] In sliding mode, the resulting equivalent control[10,11] is

$$u_{O,eq}(t) = -(GCB)^{-1}GCA\,(x(t) - \tilde{x}(t)) - w(t). \tag{5}$$

As a result, system (1) in combination with (2) and (5) can be written as

$$\dot{x}(t) = \tilde{A}x(t) + B(GCB)^{-1}GCA\tilde{x}(t) + Bu_M(t), \tag{6}$$

where

$$\tilde{A} = A - B(GCB)^{-1}GCA. \tag{7}$$

The estimated states $\tilde{x}$ as well as the nominal control signal u_M generated by the outer loop are used in (6).

Proposition 1 (OISMC[20])**.** *Suppose that Assumptions 1(a, c-e) hold and controller (4) with (3) is used. Then,*

(a) sliding is enforced from the very beginning if the scalar gain β fulfills

$$\beta(t) > \|GCB\|w_{\max} + \|GCA\|\|x(t) - \tilde{x}(t)\|; \tag{8}$$

(b) the pair $(\tilde{A}, C)$ is observable, independent of the choice of G.

Remark 1. Note that (a) means that matched perturbations are exactly eliminated starting at $t = 0$. If the number of outputs is lower or equal to the number of inputs, the resulting system in sliding mode $(\tilde{A}, C)$ is not observable.

In the work of Castanos and Fridman,[23] the goal is to stabilize the origin using measurements of the full state vector. Matrix G is chosen as the pseudoinverse B^+ of the input matrix to ensure that unmatched perturbations are not amplified by an integral sliding mode controller. In analogy, one can employ

$$G = (CB)^+ \tag{9}$$

as a weighting matrix in (3) for the case when only output information is available. Hence, the system in sliding mode is given by

$$\dot{x}(t) = \tilde{A}x(t) + B(CB)^+CA\tilde{x}(t) + Bu_M(t) \tag{10a}$$

$$y(t) = Cx(t) \tag{10b}$$

with

$$\tilde{A} = A - B(CB)^+CA. \tag{11}$$

In a next step, an observer is designed to provide estimates $\tilde{x}$.

3.1.2 | Output integral sliding mode observer

The observer structure proposed in the work of Bejarano et al[20] reconstructs in an hierarchical way the rows of the observability matrix

$$\mathcal{O} = \begin{bmatrix} C \\ C\tilde{A} \\ \vdots \\ C\tilde{A}^{l-1} \end{bmatrix} \in \mathbb{R}^{pl\times n} \tag{12}$$

so that rank($\mathcal{O}$) = n. This matrix is used to determine $\tilde{x}$ (see Figure 2). The basis for the hierarchical OISMO is formed by a Luenberger observer of the form

$$\dot{x}_L(t) = \tilde{A}x_L(t) + B(CB)^{+}CA\tilde{x}(t) + Bu_M(t) + L\left(y(t) - Cx_L\right) \tag{13}$$

for system (10). Matrix L is chosen such that the dynamics of the estimation error $\epsilon(t) = x(t) - x_L(t)$ are exponentially stable. Hence, there exist constants γ and η such that

$$\|\epsilon(t)\| \leq \gamma e^{-\eta t}\left(\mu + \|x_L(0)\|\right). \tag{14}$$

To enable reconstruction of $C\tilde{A}^j x$ for $j = 1, \ldots, l-1$, the following auxiliary dynamical systems[20] are introduced:

$$\dot{x}_a^{(j)}(t) = \tilde{A}^j x_L(t) + \tilde{A}^{j-1}B(CB)^{+}CA\tilde{x}(t) + \tilde{A}^{j-1}Bu_M(t) + \tilde{L}(C\tilde{L})^{-1}v^{(j)}(t). \tag{15}$$

Matrix $\tilde{L}$ is constant an of proper dimension. In addition, sliding variables

$$s^{(j)}(t) = \begin{cases} y(t) - Cx_a^{(1)}(t) & \text{for} \quad j = 1 \\ v_{eq}^{(j-1)}(t) + C\tilde{A}^{j-1}x_L(t) - Cx_a^{(j)}(t) & \text{for} \quad j > 1 \end{cases} \tag{16}$$

with initial values

$$s^{(j)}(0) = \begin{cases} y(0) - Cx_a^{(1)}(0) & \text{for} \quad j = 1 \\ v_{eq}^{(j-1)}(0) + C\tilde{A}^{j-1}x_L(0) - Cx_a^{(j)}(0) & \text{for} \quad j > 1 \end{cases} \tag{17}$$

and output injections

$$v^{(j)}(t) = M_j(t)\frac{s^{(j)}(t)}{\|s^{(j)}(t)\|} \tag{18}$$

with sufficiently large $M_j(t)$ are used as shown in the works of Bejarano et al.[20,21] The symbols $v_{eq}^{(j-1)}$ represent the equivalent injection terms corresponding to v_{j-1}. All rows of matrix $\mathcal{O}$ can be reconstructed using

$$\begin{cases} Cx(t) = Cx_a^{(1)}(t) \quad \text{and} \quad C\tilde{A}x(t) = C\tilde{A}x_L(t) + v_{eq}^{(1)}(t) & \text{for} \quad j = 1 \\ C\tilde{A}^j x(t) = C\tilde{A}^j x_L(t) + v_{eq}^{(j)}(t) & \text{for} \quad j > 1 \end{cases} \tag{19}$$

if sliding mode is attained. Then, (19) yields

$$Cx(t) = Cx_L(t) + Cx_a^{(1)}(t) - Cx_L(t) \tag{20a}$$

$$C\tilde{A}x(t) = C\tilde{A}x_L(t) + v_{eq}^{(1)}(t) \tag{20b}$$

$$\vdots \qquad \vdots \tag{20c}$$

$$C\tilde{A}^{l-1}x(t) = C\tilde{A}^{l-1}x_L(t) + v_{eq}^{(l-1)}(t) \tag{20d}$$

respectively

$$\mathcal{O}x(t) = \mathcal{O}x_L(t) + v_{eq}(t) \tag{21}$$

with

$$v_{eq}(t) = \begin{bmatrix} Cx_a^{(1)}(t) - Cx_L(t) \\ v_{eq}^{(1)}(t) \\ \vdots \\ v_{eq}^{(l-1)}(t) \end{bmatrix}. \tag{22}$$

Proposition 2 (OISMO[20]). *Suppose that Assumptions 1(a-e) hold. Controller (3), (4) with (8) as well as observer (13), (15) with (16) and (17) are used. The gains in (18) are tuned such that*

$$M_j(t) > \|C\tilde{A}^j\| \|x(t) - x_L(t)\|, \tag{23}$$

eg,

$$M_j(t) = \|C\tilde{A}^j\| \gamma e^{-\eta t} (\mu + \|x_L(0)\|) + \lambda \tag{24}$$

with $\lambda > 0$. Then, the plant states are exactly estimated from the very beginning, ie,

$$\tilde{x}(t) \equiv x(t) = x_L(t) + \mathcal{O}^+ v_{eq}(t) \quad \forall t \geq 0 \tag{25}$$

with $\mathcal{O}^+ = (\mathcal{O}^T\mathcal{O})^{-1}\mathcal{O}^T$, independent of time-varying matched perturbations $w(t)$.

3.1.3 | Realization of the inner loop

A realization of the hierarchical observer needs filtering to get v_{eq} such that (25) turns into

$$\tilde{x}(t) = x_L(t) + \mathcal{O}^+ v_{av}(t) \tag{26}$$

with

$$c_1 \dot{x}_{av}^{(j)}(t) + x_{av}^{(j)}(t) = v_{eq}^{(j)}(t) \tag{27}$$

using filter constant c_1. In addition, $v_{eq}^{(j)}$ has to be replaced by $v_{av}^{(j)}$ in relations (16), (17), and (22). A choice of the filter constant may be $c_1 = c\tau^\alpha$ with $0 < \alpha < 1$, $C > 0$ that is proportional to the sampling time τ of the actual discrete-time realization.[11]

One way to avoid filtering would be to make use of a technique presented in the work of Bejarano et al[24] with the drawback that the resulting control signal may be unbounded.

3.2 | Output tracking MPC

A tracking MPC formulation based on the nominal system (1) with $w(t) = 0$ is presented in this section. It will be used in the outer loop in Figure 1. A nonpathological choice of the sampling time T_S in the sense of Kalman et al[25] yields a controllable and observable discrete-time linear time-invariant plant model

$$x_{k+1} = A_d x_k + B_d u_k \tag{28a}$$

$$y_k = C x_k \tag{28b}$$

with the same dimensions as (1). One can cast the considered tracking problem into a problem of stabilizing the origin by means of a transformation using a steady-state solution (x_S, u_S) for system states and inputs. For that reason, new variables

$$\Delta x_k = x_k - x_S, \qquad \Delta u_k = u_k - u_S \qquad \text{and} \qquad \Delta y_k = y_k - y_S \tag{29}$$

are introduced yielding a €-representation of system (28)

$$\Delta x_{k+1} = A_d \Delta x_k + B_d \Delta u_k \tag{30a}$$

$$\Delta y_k = C x_k - y_S = C \Delta x_k. \tag{30b}$$

To calculate steady-state solutions (x_S, u_S) for given steady-state outputs y_S, so-called controlled variables

$$z_k = E y_k \quad \in \mathbb{R}^{N_Z} \tag{31}$$

with $N_Z m$ are used.

Assumption 2 (Rank of matrix EC)**.** Matrix $E \in \mathbb{R}^{N_Z \times p}$ is chosen such that $\text{rank}(EC) = N_Z$, ie, EC, has full rank.

Proposition 3 (Existence of steady-state solutions)**.** *Let Assumption 2 hold for discrete-time system (28) with controlled variables (31). Let y_S be an arbitrary steady-state value for outputs y_k. Then, at least one steady-state solution (x_S, u_S) exists iff*

$$\text{rank}\left(\begin{bmatrix} I_n - A_d & -B_d \\ EC & 0 \end{bmatrix}\right) = N_Z + \text{rank}\left(\begin{bmatrix} I_n - A_d & -B_d \end{bmatrix}\right). \tag{32}$$

Proof. A proof is given in the Appendix. □

Remark 2. If the solution is nonunique, additional conditions can be employed as outlined, eg, in the work of Rawlings and Mayne.[2] Modifications using an artificial reference may be applied if no feasible solution exists (see the work of Limon et al[6]).

The following assumption is imposed for this paper.

Assumption 3 (Feasible steady-state)**.** There exists at least one feasible steady-state solution (x_S, u_S) such that $x_S \in \mathbb{X}$ and $u_S \in \mathbb{U}$ for desired steady-state controlled outputs z_S and $y_S = Ez_S \in \mathbb{Y}$.

With the above assumption, an optimization problem is formulated aiming to force controlled outputs (31) in €-representation, ie,

$$\Delta z_k = E\Delta y_k = EC\Delta x_k \quad \in \mathbb{R}^{N_Z}, \tag{33}$$

to zero. An iterative solution of (30) and (33) for a prediction horizon N and control horizon $N_C \leq N$ yields

$$\Delta \bar{x}_{k+1} = F_X \Delta x_k + H_X \Delta \bar{u}_k \tag{34a}$$

$$\Delta \bar{z}_{k+1} = F \Delta x_k + H \Delta \bar{u}_k, \tag{34b}$$

where matrices F, F_X, H, and H_X only depend on A_d, B_d, C, and both horizons.[2,4] Predicted states and controlled outputs

$$\Delta \bar{x}_{k+1} = \begin{bmatrix} \Delta \hat{x}_{k+1} \\ \Delta \hat{x}_{k+2} \\ \vdots \\ \Delta \hat{x}_{k+N} \end{bmatrix} \in \mathbb{R}^{nN}, \qquad \Delta \bar{z}_{k+1} = \begin{bmatrix} \Delta \hat{z}_{k+1} \\ \Delta \hat{z}_{k+2} \\ \vdots \\ \Delta \hat{z}_{k+N} \end{bmatrix} \in \mathbb{R}^{N_Z N} \tag{35}$$

depend on the vector of optimization variables

$$\Delta \bar{u}_k = \begin{bmatrix} \Delta \hat{u}_k \\ \Delta \hat{u}_{k+1} \\ \vdots \\ \Delta \hat{u}_{k+N_C-1} \end{bmatrix} \in \mathbb{R}^{mN_C}, \tag{36}$$

where $\Delta \hat{x}_{k+i} = \phi_{k+i}(\Delta x_k, \Delta \bar{u}_k)$ is the solution of (30) at step $k+i$ starting with initial condition €x_k (29). The references $r = z_S \in \mathbb{R}^{N_Z}$ to be tracked are assumed to be constant over the prediction horizon. A quadratic cost function of form

$$V_N(\Delta x_k, \Delta \bar{u}_k) = \sum_{i=0}^{N-1} \Delta \hat{z}_{k+i}^T Q \Delta \hat{z}_{k+i} + \sum_{i=0}^{N_C-1} \Delta \hat{u}_{k+i}^T R \Delta \hat{u}_{k+i} + \Delta \hat{z}_{k+N}^T Q_f \Delta \hat{z}_{k+N} \tag{37}$$

or alternatively

$$V_N(\Delta x_k, \Delta \bar{u}_k) = \sum_{i=0}^{N-1} \Delta \hat{x}_{k+i}^T P \Delta \hat{x}_{k+i} + \sum_{i=0}^{N_C-1} \Delta \hat{u}_{k+i}^T R \Delta \hat{u}_{k+i} + \Delta \hat{x}_{k+N}^T P_f \Delta \hat{x}_{k+N} \tag{38}$$

can be used with terminal cost $V_f(\Delta \hat{x}_{k+N}) = \Delta \hat{x}_{k+N}^T P_f \Delta \hat{x}_{k+N}$. The matrices

$$P = C^T Q C \qquad \text{and} \qquad P_f = C^T Q_f C \tag{39}$$

are positive semidefinite for $Q \geq 0$, $Q_f \geq 0$ and $p < n$. Therefore, cost function (38) with weights P is used instead of (37) with weights Q as will be shown later. Cost function (38) is minimized subject to hard constraints

$$\hat{u}_{k+i} \in \mathbb{U}, \qquad \hat{x}_{k+i} \in \mathbb{X}, \qquad \hat{y}_{k+i} \in \mathbb{Y} \qquad \text{for all} \qquad i \in \mathbb{I}_{\geq 0} \tag{40}$$

according to Assumption 1(f) and a terminal constraint set

$$\Delta\hat{x}_{k+N} \in \delta\mathbb{X}_f \tag{41}$$

to ensure stability as will be shown in the next section.

3.3 | Analysis of the overall system

The stability of the closed loop consisting of the inner loop with an OISMC, an OISMO, and the outer loop with a tracking MPC as shown in Figure 1 is investigated in this section.

Theorem 1 (Stability of the overall system)**.** *Let Assumptions 1 and 3 hold. The closed loop consists of*

(a) plant (1) with constraints $u \in \mathbb{U}$, $x \in \mathbb{X}$ and $y \in \mathbb{Y}$;
(b) the inner loop with

- *an OISM controller (3), (4) tuned such that relations (8) and (9) are fulfilled;*
- *an OISM observer (13), (15)-(17) with L chosen such that matrix $(\tilde{A} - LC)$ is Hurwitz and (24) is satisfied with $\lambda > 0$;*

(c) the outer loop with an output tracking MPC with prediction horizon N, control horizon N_C, cost function (38) and

- *a nominal control signal $u_{M,k}$ constrained by*

$$\mathbb{U}_M = \left\{ u_{M,k+i} = u_{k+i} - \max_t \beta(t)\, \mathrm{sign} u_{k+i} \quad | \quad u_{k+i} \in \mathbb{U} \right\} \quad \forall i \in \mathbb{I}_{\geq 0}; \tag{42}$$

- *symmetric positive definite weighting matrices $P > 0$ and $R > 0$;*
- *terminal constraint set $\delta\mathbb{X}_f$ for $\Delta\hat{x}_{k+N}$ that is chosen as the maximal admissible set for the corresponding unconstrained infinite horizon problem*
- *matrix P_f in the terminal cost is chosen as the solution of the discrete algebraic Riccati equation*

$$P_f = P + A_d^T P_f A_d - A_d^T P_f B_d \left(B_d^T P_f B_d + R_N \right)^{-1} B_d^T P_f A_d \tag{43}$$

with

$$R_N = \begin{cases} 0 & \text{if} \quad N_C < N \\ R & \text{if} \quad N_C = N \end{cases}. \tag{44}$$

Then, independently of matched bounded perturbations $w(t)$, exponential tracking of constant references is achieved.

Proof. A proof is given in the Appendix. □

4 | EXPERIMENTAL RESULTS

A second-order mechanical system, called Pendubot,[26] is used to show the properties of the proposed approach.

4.1 | Mathematical model

Figure 3 shows a sketch as well as a photo of the considered lab experiment. It consists of an inner link that is actuated via a DC motor and an unactuated outer link. The desired motor current represents the input variable $u(t)$ of the system. An additional loop, to control the motor voltage such that the desired current is achieved, is realized by means of an electronic circuit. This current control loop is neglected for the modeling given below. The lab experiment is connected via Quanser QuaRC real-time control software[27] to the computer, where MATLAB[28] is used to implement the presented observer and

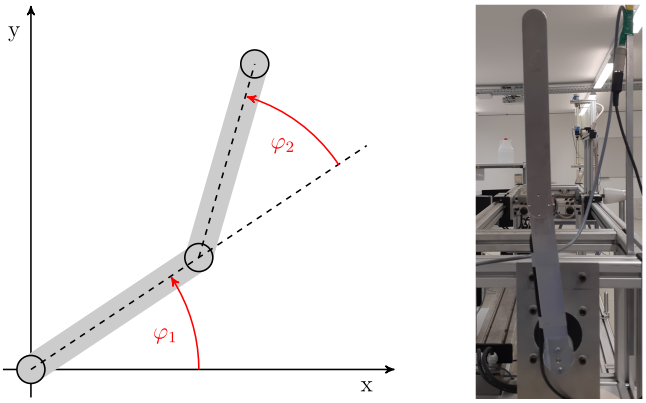

FIGURE 3 Sketch and photo of the Pendubot lab experiment [Colour figure can be viewed at wileyonlinelibrary.com]

TABLE 1 Parameter of the Pendubot lab experiment

$a_{21} = 48.4630s^{-1}$	$a_{22} = 2.3246$	$a_{23} = 21.5091s^{-1}$	$a_{24} = 0.1929$	$b_2 = 8.2696A^{-1}$
$a_{41} = 50.5217s^{-1}$	$a_{42} = 5.2073$	$a_{43} = 106.2215s^{-1}$	$a_{44} = 0.7202$	$b_4 = 18.5246A^{-1}s^{-1}$

controllers. For the inner loop shown in Figure 1, $\tau = 1$ ms is used as sampling time for the OISM observer and controller. It is the smallest possible time instant for the present hardware setup. In contrast, sampling time $T_S = 25$ ms is selected for the outer loop to provide enough time for the optimization algorithm to solve the quadratic MPC problem.

Using Lagrange equations, a nonlinear model can be derived as, eg, shown in the work of Altenbuchner.[26] Angles φ_1 and φ_2 shown in Figure 3 and the corresponding angular velocities are used as generalized coordinates, so that the state vector is given by

$$x = \begin{bmatrix} \varphi_1 \\ \dot{\varphi}_1 \\ \varphi_2 \\ \dot{\varphi}_2 \end{bmatrix}. \tag{45}$$

Linearization in $x_E = \begin{bmatrix} \pi/2 & 0 & 0 & 0 \end{bmatrix}^T$ and $u_E = 0$ (up-up position, ie, both links point upwards) yields system matrices

$$A = \begin{bmatrix} 0 & 1 & 0 & 0 \\ a_{21} & a_{22} & a_{23} & a_{24} \\ 0 & 0 & 0 & 1 \\ a_{41} & a_{42} & a_{43} & a_{44} \end{bmatrix} \quad \text{and} \quad B = \begin{bmatrix} 0 \\ b_2 \\ 0 \\ b_4 \end{bmatrix} \tag{46}$$

with parameters listed in Table 1. The measurement signals are given by the position of the inner link and the velocity of the outer link such that

$$C = \begin{bmatrix} 1 & 0 & 0 & 0 \\ 0 & 0 & 0 & 1 \end{bmatrix}. \tag{47}$$

Box constraints

$$20A = u_{\min} \leq u(t) \leq u_{\max} = 20A \tag{48a}$$

$$\begin{bmatrix} -20^\circ & -1 & -20^\circ & -1 \end{bmatrix}^T = x_{\min} \leq x(t) \leq x_{\max} = \begin{bmatrix} 20^\circ & 1 & 20^\circ & 1 \end{bmatrix}^T \tag{48b}$$

$$y_{\min} = Cx_{\min} \leq y(t) \leq y_{\max} = Cx_{\max} \tag{48c}$$

are used for all subsequent experiments.

4.2 | Parameters for observer and controllers

For the performed experiments, a disturbance

$$w(t) = w_0 + w_1 \sin(50t) + w_2 \sin\left(\sqrt{200t}\right) \tag{49}$$

consisting of two sinusoidal components and offset is used, where $w_{\max} = 4$. The OISM controller and OISM observer are tuned as $\beta = 5$ and $M = 50$, $c_1 = 50\tau^{4/5}$ respectively. The parameters for the tracking MPC are $N = 6$, $N_C = 4$, $Q = \text{diag}([100\ 1\ 100\ 1])$, and $R = 1$. Matrix $E = [1\ \ 0]$ is chosen such that (3) is fulfilled and steady states (x_S, u_S) can be calculated. The resulting quadratic program is solved by means of qpOASES.[29]

The maximal admissible set $\delta\mathbb{X}_f$ for the unconstrained problem for system

$$\Delta x_{k+1} = (A_d + B_d K)\Delta x_k \tag{50a}$$

$$\Delta y_k = C\Delta x_k \tag{50b}$$

with constraints $\Delta x_k \in \delta\mathbb{X}$, $\Delta u_k \in \delta\mathbb{U}_M$, and $\Delta y_k \in \delta\mathbb{Y}$ is calculated using algorithm 3.2 from the work of Gilbert and Tan[30] for three different cases: system matrix $A_d + B_d K$ and (i) output matrix K for constraints in $€u_M = u_{k,M} - u_S$, (ii) output matrix I for constraints in $€x_k = x_k - x_S$, and (iii) output matrix C for constraints in $€y_k = y_k - y_S$. Finally, the intersection of these sets from (i) to (iii) gives $\delta\mathbb{X}_f$ denoted by

$$U\Delta x_k \leq V. \tag{51}$$

For the construction of the region $\delta\mathcal{X}_N$ where a solution of the MPC problem exists, constraints for predicted inputs, states, and outputs (34) as well as the terminal set $\delta\mathbb{X}_f$ are combined to

$$\begin{bmatrix} 0_{mN_C\times n} \\ 0_{mN_C\times n} \\ -I_n \\ I_n \\ -F_X \\ F_X \\ -C \\ C \\ -F \\ F \\ UF_f \end{bmatrix} \Delta x_k + \begin{bmatrix} -I_{mN_C} \\ I_{mN_C} \\ 0_{n\times mN_C} \\ 0_{n\times mN_C} \\ -H_X \\ H_X \\ 0_{p\times mN_C} \\ 0_{p\times mN_C} \\ -H \\ H \\ UH_f \end{bmatrix} \Delta\bar{u}_k \leq \begin{bmatrix} -\bar{u}_{\min} + \bar{u}_S \\ +\bar{u}_{\max} - \bar{u}_S \\ -x_{\min} + x_S \\ x_{\max} - x_S \\ -\bar{x}_{\min} + F_X x_S + H_X \bar{u}_S \\ \bar{x}_{\max} - F_X x_S - H_X \bar{u}_S \\ -y_{\min} + Cx_S \\ y_{\max} - Cx_S \\ -\bar{y}_{\min} + Fx_S + H\bar{u}_S \\ \bar{y}_{\max} - Fx_S - H\bar{u}_S \\ V \end{bmatrix}, \tag{52}$$

where F_f and H_f are submatrices of F_X and H_X (last n rows). Symbols $I_{r\times c}$ and $0_{r\times c}$ stand for identity and zero matrices with r rows and c columns. Vectors $\bar{u}_S$ respectively $\bar{x}_S$ correspond to the N_C-times concatenation of u_S respectively the N-times concatenation of x_S. A projection onto Δx_k gives $\delta\mathcal{X}_N$. The multiparametric toolbox 3.0,[31] was used to remove redundant inequalities and perform set projections.

Figure 4 shows examples for sets $\delta\mathbb{X}_f$ (red) and $\delta\mathcal{X}_N$ (green). Since the considered system is of order $n = 4$, always one component of the state vector is kept constant, while regions for the other three states are drawn in the subfigures for $z_S = 10°$. Please note that the volume of $\delta\mathcal{X}_N$ is not significantly larger than the volume of $\delta\mathbb{X}_f$ due to the properties of the Pendubot in the unstable upward position (up-up position). The volume of set $\delta\mathcal{X}_N$ is 41.7% larger compared to the volume of $\delta\mathbb{X}_f$. In the next sections, the proposed approach is tested in simulation as well as on the lab experiment.

4.3 | Simulation results

The effect of the chosen sampling time τ for the inner control loop (see Figure 1) and filter constant c_1 in (27) is investigated in simulation. Note that constant c is shown in the legends of Figures 5 to 7 instead of $c_1 c\tau_\alpha$, where $\alpha = 4/5$ is chosen. These figures show typical results for the estimation of x_1 and x_2 when only MPC (left plots) respectively MPC with the inner OISM controller (MPS) is used (right plots) for initial condition $x(0) = \begin{bmatrix} x_{1,\max} & x_{2,\min} & x_{3,\min} & x_{4,\max} \end{bmatrix}^T$. In both cases, the MPC uses the actual (simulated) values for the states to be able to interpret the behavior of the OISM observer independently of the chosen configuration of the closed loop. The sampling time of the outer loop is $T_S = 25$ ms for all investigations.

Figures 5 and 6 depict the dependency of the estimation errors $e_1 = x_1 - \tilde{x}_1$ respectively $e_2 = x_2 - \tilde{x}_2$ on different settings for c with $\tau = 1$ ms. It can be clearly seen that state x_1 can be estimated from the very beginning for all c, whereas the estimation of x_2 improves for smaller c. Conversely, the amplitude of the resulting oscillations is increased due to weaker

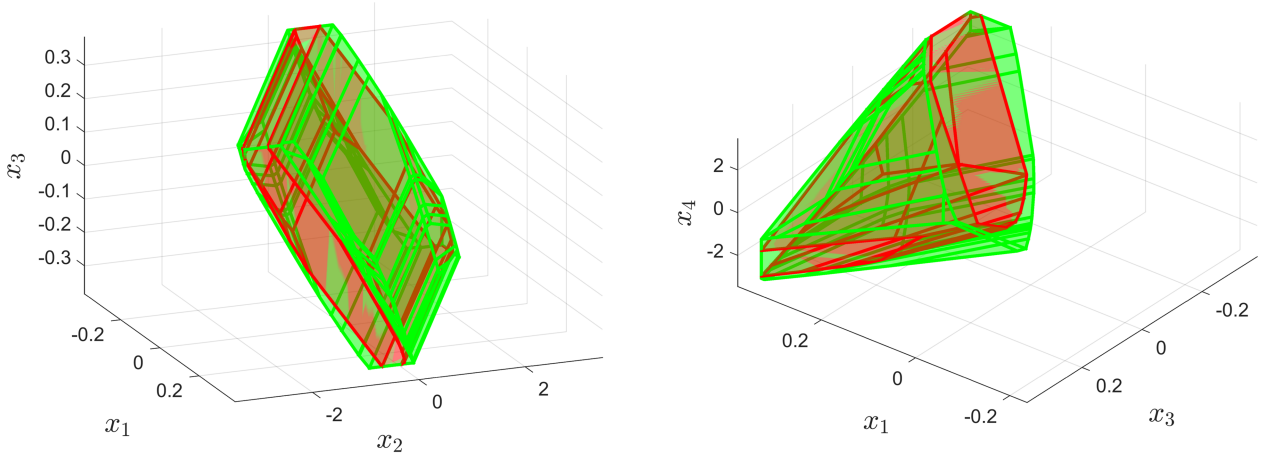

FIGURE 4 Examples for maximal admissible set $\delta\mathbb{X}_f$ (red) and the region where a solution to the model predictive control problem exist $\delta\mathcal{X}_N$ (green) for $x_4 = -0.3$ (left plot) and $x_2 = -2$ (right plot) respectively [Colour figure can be viewed at wileyonlinelibrary.com]

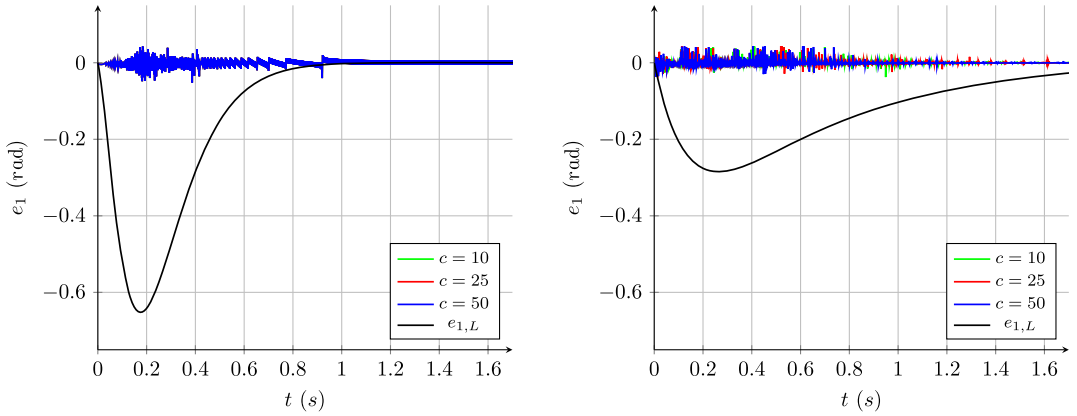

FIGURE 5 Observation error for the first (measured) state x_1 for different filter constants c. Left: with model predictive control only. Right: with model predictive sliding. Note that the results are similar for all considered c [Colour figure can be viewed at wileyonlinelibrary.com]

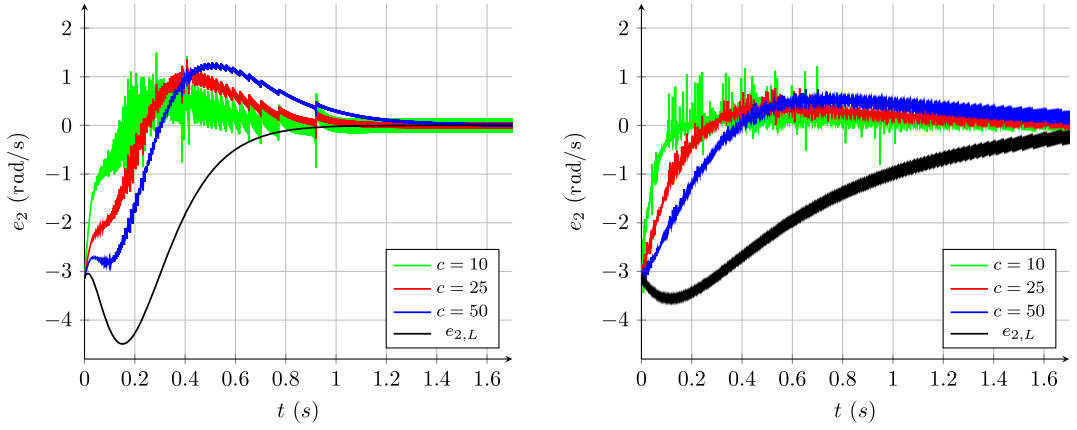

FIGURE 6 Observation error for the second (not measured) state x_2 for different filter constants c. Left: with model predictive control only. Right: with model predictive sliding [Colour figure can be viewed at wileyonlinelibrary.com]

filtration (27) for the calculation of the equivalent injection terms in the observer. Variables $e_{1,L} = x_1 - x_{1,L}$ respectively $e_{2,L} = x_2 - x_{2,L}$ represent the error using a Luenberger observer only (see Figure 2).

Figure 7 shows the dependency of e_2 on different settings for sampling time τ with fixed filter constant $c = 50$, which is chosen as trade-off between convergence time and the amplitude of the oscillations.

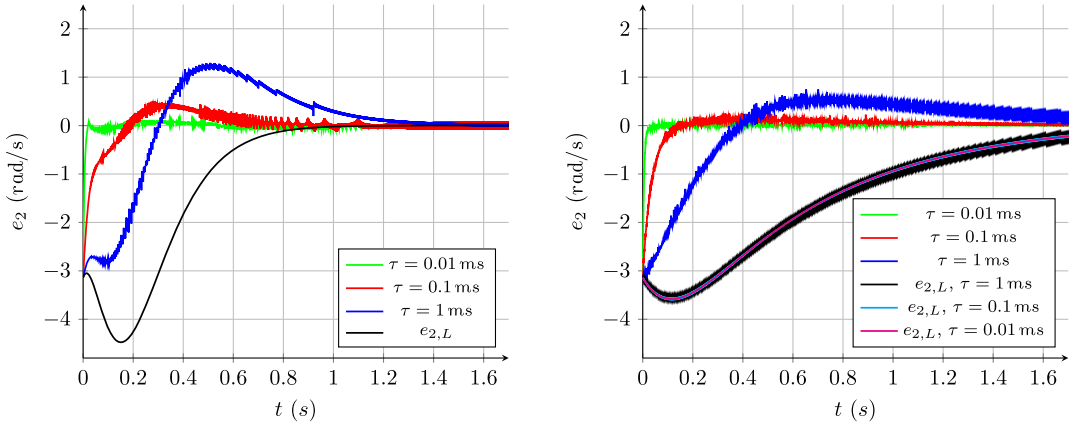

FIGURE 7 Observation error for the second (not measured) state x_2 for different sampling times τ for the inner control loop. Left: with model predictive control only. Right: with model predictive sliding [Colour figure can be viewed at wileyonlinelibrary.com]

As expected, a smaller sampling time significantly improves the performance leading to the exact compensation for $\tau \to 0$. In the left plot of Figure 7, signal $x_{2,L}$ depends on τ as well. This is due to (13) where $\tilde{x}$ is considered in the Luenberger observer as an external input to be able to observe the inner loop while sliding. This effect is not visible when no inner control loop is used (see left plot in Figure 7).

4.4 | Experimental results

The combination of tracking MPC, OISM controller, and OISM observer is tested at the Pendubot lab experiment shown in Figure 3 (right). In all subsequent experiments, a set point changes between $z_S = -10°$ and $z_S = -10°$ starting from $z_S = -10°$ is performed.

Figure 8 (left) shows results using MPC only, where estimates of the states are provided by the presented OISM observer. The blue curve illustrates the behavior without additional perturbation, ie, only unmodeled parts and external vibrations act as disturbances. Spikes in the opposite directions during abrupt changes of the set point appear due to the nonminimum phase property of the considered system. When disturbance (49) is used in addition, one can see clear deviations (Figure 8, red) from the desired values shown in black. The experiment is stopped at time $t \approx 17.5$ seconds because x_1 leaves the admissible region.

In the right plot of Figure 8, these results are compared to experimental data achieved with the proposed MPS algorithm. The results are clearly better even in the case without additional perturbation, ie, $w(t) = 0$ (red). Note that the tracking performance is quite similar in the case of $w(t) \neq 0$. The corresponding control signals u_0 for the OISM controller, u_M for the MPC, and their sum u is shown in Figure 9 (left) for a smaller time interval. The right plot of Figure 9 depicts the

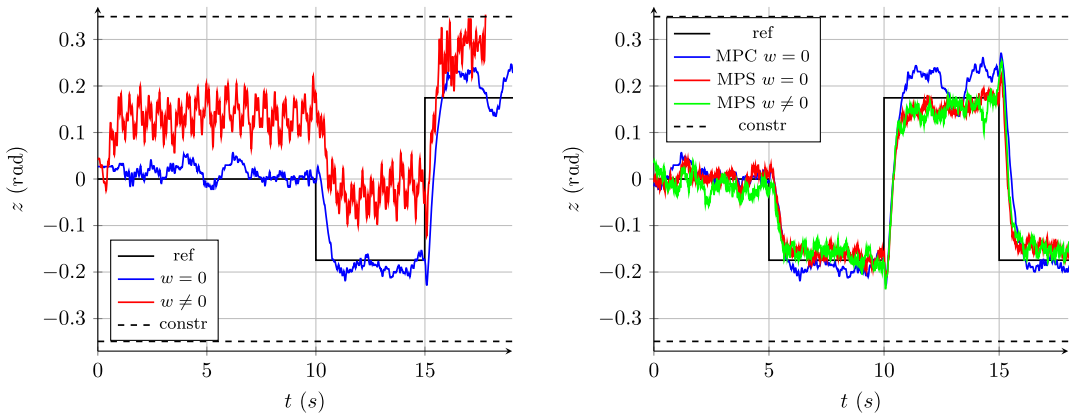

FIGURE 8 Left: Tracking performance using model predictive control (MPC) only without disturbance (blue) and with disturbance $w(t) \neq 0$ (red). Right: Comparison of the tracking performance using MPC only without disturbance (blue) and the proposed model predictive sliding (MPS) approach without (red) and with disturbance $w(t) \neq 0$ (green) [Colour figure can be viewed at wileyonlinelibrary.com]

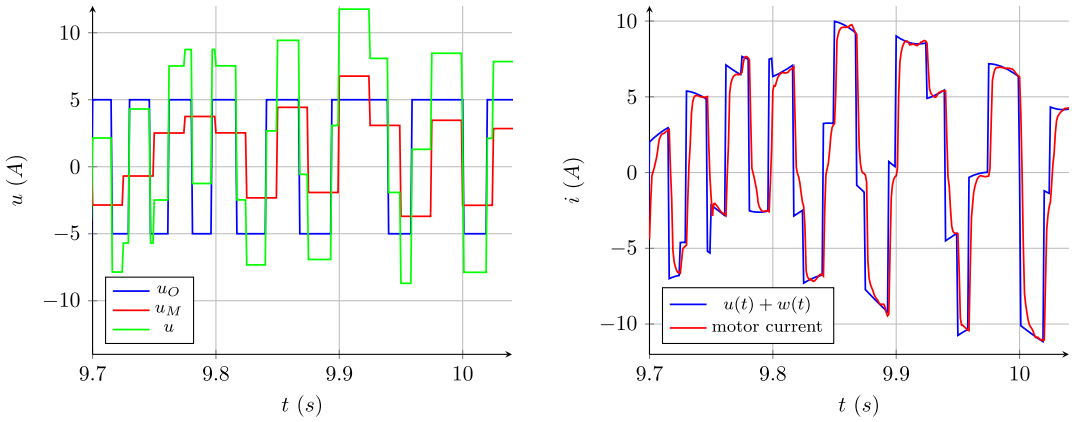

FIGURE 9 Left: Actuating signal provided by the algorithm for the case with $w(t) \neq 0$. Right: Corresponding input to the actuator and actual current at the DC motor [Colour figure can be viewed at wileyonlinelibrary.com]

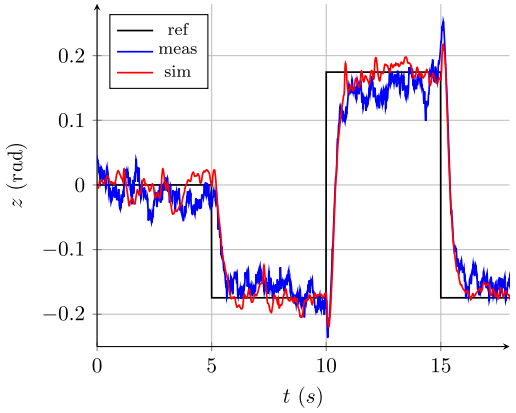

FIGURE 10 Comparison of measurements with simulation results for the case with $w(t) \neq 0$ [Colour figure can be viewed at wileyonlinelibrary.com]

effects in the current control loop that is implemented in hardware at the lab experiment. The blue curve represents the input to the actuator, and the red curve represents the actual current at the DC motor. This difference due to actuator dynamics is neither modeled nor taken into account for controller design.

Finally, Figure 10 shows a comparison of the tracking performance between simulation and real-world measurements for the case with additional perturbation. This good matching is achieved even though multiple effects, such as the actuator dynamics of the DC motor and the friction in the joints, are neglected in the modeling.

5 | CONCLUSION AND OUTLOOK

This paper presents a method to robustly track the outputs of constrained linear systems exploiting the properties of OISMs as well as MPC. An excess of the number of outputs compared to the number of matched perturbations is necessary to be able to exactly reconstruct the system states independent of matched (time-varying) perturbation. Issues due to the actual implementation of the algorithm were shown in simulation and using an unstable mechanical lab experiment.

Future work will focus on the extension of the approach to unmatched perturbations and on methods to smooth the control signal provided by the inner loop using, eg, the saturated super-twisting algorithm[32,33] granted that the actuators are fast enough, as shown in the work of Pérez-Ventura and Fridman.[34] Also explicit MPC formulations[1] are of great interest for further improvement of the real-time capability.

ACKNOWLEDGEMENTS

We gratefully acknowledge the financial support of (i) the Christian Doppler Research Association, the Austrian Federal Ministry for Digital and Economic Affairs, and the National Foundation for Research, Technology and Development; (ii) CONACYT (Consejo Nacional de Ciencia y Tecnologia) under grant 282013; PAPIIT-UNAM (Programa de Apoyo a Proyectos de Investigación e Innovación Tecnológica) under grant IN 115419; and (iii) the European Unions Horizon 2020 research and innovation programme under the Marie Skłodowska-Curie under grant agreement No. 734832.

ORCID

M. Steinberger https://orcid.org/0000-0001-6545-3949
I. Castillo https://orcid.org/0000-0001-6267-0841
L. Fridman https://orcid.org/0000-0003-0208-3615

REFERENCES

1. Borrelli F, Bemporad A, Morari M. *Predictive Control for Linear and Hybrid Systems*. Cambridge, UK: Cambridge University Press; 2017.
2. Rawlings JB, Mayne D. *Model Predictive Control: Theory and Design*. Los Gatos, CA: Nob Hill Publishing; 2016.
3. Fernandez-Camacho EF, Bordons-Alba C. *Model Predictive Control*. London, UK: Springer; 2007.
4. Maciejowski J. *Predictive Control With Constraints*. London, UK: Pearson; 2002.
5. Mayne D, Rawlings JB, Rao CV, Scokaert POM. Constrained model predictive control: stability and optimality. *Automatica*. 2000;36:789-814.
6. Limon D, Alvarado I, Alamo T, Camacho EF. MPC for tracking piecewise constant references for constrained linear systems. *Automatica*. 2008;44:2382-2387.
7. Mayne D, Falugi P. Generalized stabilizing conditions for model predictive control. *J Optim Theory Appl*. 2016;169(3):719-734.
8. Mayne D. Model predictive control: recent developments and future promise. *Automatica*. 2014;50:2967-2986.
9. Shtessel Y, Edwards C, Fridman L, Levant A. *Sliding Mode Control and Observation*. Basel, Switzerland: Birkhäuser; 2013.
10. Edwards C, Spurgeon S. *Sliding Mode Control: Theory and Applications*. London, UK: Taylor & Francis; 1998.
11. Utkin V. *Sliding Modes in Control and Optimization*. New York, NY: Springer; 1992.
12. Garcia-Gabin W, Zambrano D, Camacho EF. Sliding mode predictive control of a solar air conditioning plant. *Control Eng Pract*. 2009;17(6):652-663.
13. Perez M, Jimenez E, Camacho EF. Robust stability analysis and tuning of a predictive sliding mode controller. *Eur J Control*. 2010;16(3):275-288.
14. Errouissi R, Yang J, Chen W-H, Al-Durra A. Robust nonlinear generalised predictive control for a class of uncertain nonlinear systems via an integral sliding mode approach. *Int J Control*. 2016;89(8):1698-1710.
15. Utkin V, Shi J. Integral sliding mode in systems operating under uncertainty conditions. In: Proceedings of the 35th IEEE Conference on Decision and Control; 1996; Kobe, Japan.
16. Rubagotti M, Raimondo DM, Ferrara A, Magni L. Robust model predictive control with integral sliding mode in continuous-time sampled-data nonlinear systems. *IEEE Trans Autom Control*. 2011;56(3):556-570.
17. Raimondo DM, Rubagotti M, Jones CN, Magni L, Ferrara A, Morari M. Multirate sliding mode disturbance compensation for model predictive control. *Int J Robust Nonlinear Control*. 2015;25(16):2984-3003.
18. Utkin V, Guldner J, Shi J. *Sliding Mode Control in Electromechanical Systems*. London, UK: Taylor & Francis; 1999.
19. Steinberger M, Castillo I, Horn M, Fridman L. Model predictive output integral sliding mode control. In: Proceedings of the 14th International Workshop on Variable Structure Systems; 2016; Nanjing, China.
20. Bejarano FJ, Fridman L, Poznyak A. Output integral sliding mode control based on algebraic hierarchical observer. *Int J Robust Nonlinear Control*. 2007;80(3):443-453.
21. Fridman L, Poznyak A, Bejarano FJ. *Robust Output LQ Optimal Control via Integral Sliding Modes*. Basel, Switzerland: Birkhäuser; 2014.
22. Filippov AF. *Differential Equations with Discontinuous Righthand Dides*. Dordrecht, The Netherlands: Springer; 1988. *Mathematics and Its Applications*; vol. 18.
23. Castanos F, Fridman L. Analysis and design of integral sliding manifolds for systems with unmatched perturbations. *IEEE Trans Autom Control*. 2006;51(5):853-858.
24. Bejarano FJ, Fridman L, Poznyak A. Exact state estimation for linear systems with unknown inputs based on hierarchical super-twisting algorithm. *Int J Control*. 2007;17(18):1734-1753.
25. Kalman R, Ho BL, Narendra N. Controllability of linear dynamical systems. *Contrib Differ Equ*. 1963;1:198-213.
26. Altenbuchner M. *Aufbau und Regelung des Labormodells Pendubot* [master's thesis]. Graz, Austria: Graz University of Technology; 2007.
27. Quanser. QuaRC real-time control software. https://www.quanser.com. Accessed August 16, 2018.
28. Mathworks. MATLAB for Artificial Intelligence. https://www.mathworks.com. Accessed August 16, 2018.
29. Ferreau HJ, Kirches C, Potschka A, Bock HG, Diehl M. qpOASES: a parametric active-set algorithm for quadratic programming. *Math Program Comput*. 2014;6(4):327-363.
30. Gilbert EG, Tan KTT. Linear systems with state and control constraints: the theory and application of maximal output admissible sets. *IEEE Trans Autom Control*. 1991;36(9):1008-1020.

31. Herceg M, Kvasnica M, Jones CN, Morari M. Multi-parametric toolbox 3.0. In: Proceedings of the European Control Conference; 2013; Zürich, Switzerland. https://control.ee.ethz.ch/~mpt
32. Castillo I, Steinberger M, Fridman L, Moreno JA, Horn M. Saturated super-twisting algorithm: Lyapunov based approach. Paper presented at: 14th International Workshop on Variable Structure Systems; 2016; Nanjing, China.
33. Castillo I, Steinberger M, Fridman L, Moreno J, Horn M. Saturated super-twisting algorithm based on perturbation estimator. Paper presented at: 14th International Workshop on Variable Structure Systems; 2016; Nanjing, China.
34. Pérez-Ventura U, Fridman L. When is it reasonable to implement the discontinuous sliding-mode controllers instead of the continuous ones? Frequency domain criteria. *Int J Robust Nonlinear Control*. 2019;29(3):810-828.

How to cite this article: Steinberger M, Castillo I, Horn M, Fridman L. Robust output tracking of constrained perturbed linear systems via model predictive sliding mode control. *Int J Robust Nonlinear Control*. 2020;30:1258–1274. https://doi.org/10.1002/rnc.4826

APPENDIX A

PROOF OF PROPOSITION 3

A steady-state solution of (28) has to fulfill

$$x_S = A_d x_S + B_d u_S \tag{A1}$$

$$y_S = C x_S \tag{A2}$$

respectively

$$\underbrace{\begin{bmatrix} I_n - A_d & -B_d \\ C & 0 \end{bmatrix}}_{Z_C} \begin{bmatrix} x_S \\ u_S \end{bmatrix} = \begin{bmatrix} 0 \\ y_S \end{bmatrix}. \tag{A3}$$

According to Rawlings and Mayne,[2] such a solution exists iff the rows of Z_C are linearly independent which is possible only for $p \leq m$. If $p > m$ at least two rows are linearly dependent. As a consequence, only references for controlled variables (31) have to be chosen such that

$$\underbrace{\begin{bmatrix} I_n - A_d & -B_d \\ EC & 0 \end{bmatrix}}_{Z} \begin{bmatrix} x_S \\ u_S \end{bmatrix} = \begin{bmatrix} 0 \\ z_S \end{bmatrix}, \tag{A4}$$

where z_S symbolizes the steady-state solution of the controlled variables. This is true in the general case in which the vector on the right-hand side can be arbitrary. In the present formulation, the first n elements are zero. Therefore, the mentioned condition is sufficient but not necessary.

In the first n rows, a rank deficiency $n - \text{rank}([I_n - A_d - B_d])$ is admissible because of the zeros on the right-hand side. As a consequence, matrix Z must have rank $n + N_Z$ minus the rank deficiency in the upper part, ie,

$$\text{rank}\, Z = n + N_Z - (n - \text{rank}\,([I_n - A_d \quad -B_d])). \tag{A5}$$

APPENDIX B

PROOF OF THEOREM 1

Stability of the inner loop follows immediately by Propositions 1 and 2 as outlined in the work of Bejarano et al.[20] Because of Proposition 2, $\hat{x}(t) \equiv x(t)$ and therefore (10) turns into

$$\dot{x}(t) = Ax(t) + Bu_M(t) \tag{B1a}$$

$$y(t) = Cx(t), \tag{B1b}$$

which is the original system without perturbation. A pathological choice of the sampling time T_S yields a controllable and observable discrete-time linear time-invariant plant model in the €-representation, ie,

$$\Delta x_{k+1} = A_d \Delta x_k + B_d \Delta u_k \tag{B2a}$$

$$\Delta y_k = C x_k, \tag{B2b}$$

with $€u_k = u_{M,k} - u_S$. In addition, the constraints are reformulated in terms of this €-representation leading to

$$\Delta \hat{x}_{k+i} \in \delta\mathbb{X} = \left\{ \Delta x_j = x_j - x_S \quad | \quad x_j \in \mathbb{X}, \quad Cx_j \in \mathbb{Y}, \quad \forall j \in \mathbb{I}_{\geq 0} \right\} \tag{B3a}$$

$$\Delta \hat{y}_{k+i} \in \delta\mathbb{Y} = \left\{ \Delta y_j = C\Delta x_j \quad | \quad \Delta x_j \in \delta\mathbb{X}, \quad \forall j \in \mathbb{I}_{\geq 0} \right\} \tag{B3b}$$

$$\Delta \hat{u}_{k+i} \in \delta\mathbb{U}_M = \left\{ \Delta u_j = u_j - u_S - \max_t \beta(t) \operatorname{sign} u_j \quad | \quad u_j \in \mathbb{U}, \quad \forall j \in \mathbb{I}_{\geq 0} \right\} \tag{B3c}$$

respectively

$$\Delta \hat{x}_{k+N} \in \delta\mathbb{X}_f \subseteq \delta\mathbb{X}. \tag{B4}$$

The set of states in $\delta\mathbb{X}$ for which a solution exists is given by

$$\delta\mathcal{X}_N = \left\{ \Delta x_k \in \mathbb{R}^n \quad | \quad \exists \Delta \bar{u}_k \in \mathbb{R}^{mN} \text{ such that } (\Delta x_k, \Delta \bar{u}_k) \in \delta\mathbb{Z}_N \right\} \tag{B5}$$

with

$$\delta\mathbb{Z}_N = \left\{ (\Delta x_k, \Delta \bar{u}_k) \quad | \quad \Delta \hat{u}_{k+i} \in \delta\mathbb{U}_M, \ \phi_{k+i}(\Delta x_k, \Delta \bar{u}_k) \in \delta\mathbb{X}, \quad \forall i \in \mathbb{I}_{0:N-1} \quad \text{and} \right. \tag{B6}$$

$$\left. \phi_{k+N}(\Delta x_k, \Delta \bar{u}_k) \in \delta\mathbb{X}_f \right\}. \tag{B7}$$

This means that $\delta\mathcal{X}_N$ is a set of states $€x_k$ can be steered in N steps or less by an admissible control sequence to $\delta\mathbb{X}_f$. All δ-sets are also compact due to Assumption 1(f).

As a consequence, one can follow the line of the proof stated in the work of Mayne et al.[5] The continuity of system and cost together with the properties of constraint sets ensure the existence of solutions to the optimal control problem (see the work of Rawlings and Mayne[2]). Value function $V_N^*(\Delta x_k) = V_N(\Delta x_k, \Delta \bar{u}_k^*)$, ie, the cost function in the optimum, is used as a Lyapunov function candidate with $V_N^*(0) = 0$, $V_N^*(\Delta x_k) \geq \Delta x_k^T P \Delta x_k > 0$ for all $\Delta x_k \neq 0$ and $V_N^*(\Delta x_k) \to \infty$ for $\|\Delta x_k\| \infty$. Vector

$$\Delta \bar{u}_k^* = \begin{bmatrix} \Delta \hat{u}_k^* \\ \Delta \hat{u}_{k+1}^* \\ \vdots \\ \Delta \hat{u}_{k+N_C-1}^* \end{bmatrix} \tag{B8}$$

represents the optimal control sequence for the current iteration. This yields

$$\begin{aligned} V_N^*(\Delta x_k) = V_N(\Delta x_k, \Delta \bar{u}_k^*) = \Delta x_k^T P \Delta x_k + \Delta \hat{u}_k^{*T} R \Delta \hat{u}_k^* \\ + \sum_{i=1}^{N-1} \Delta \hat{x}_{k+i}^{*T} P \Delta \hat{x}_{k+i}^* + \sum_{i=1}^{N_C-1} \Delta \hat{u}_{k+i}^{*T} R \Delta \hat{u}_{k+i}^* + \Delta \hat{x}_{k+N}^{*T} P_f \Delta \hat{x}_{k+N}^*. \end{aligned} \tag{B9}$$

The value function for the next iteration can be upper bounded[2] by

$$V_N^*(\Delta x_{k+1}) = V_N\left(\Delta x_{k+1}, \Delta \bar{u}_k^*\right) \leq V_N\left(\Delta x_{k+1}, \Delta \bar{u}_{k+1}\right), \tag{B10}$$

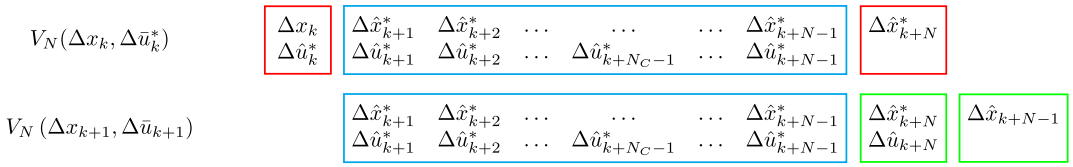

FIGURE B1 Time evolution of the cost function for initial times k and $k+1$. Entries $\Delta\hat{u}_{k+i}$ for $i = N_C, N_C+1, \ldots, N$ are zero whenever $N_C < N$. Red parts are removed, green parts are added in (B12) [Colour figure can be viewed at wileyonlinelibrary.com]

where

$$\Delta\bar{u}_{k+1} = \begin{bmatrix} \Delta\hat{u}_{k+1}^* \\ \Delta\hat{u}_{k+2}^* \\ \vdots \\ \Delta\hat{u}_{k+N_C-1}^* \\ \Delta\hat{u} \end{bmatrix} \in \mathbb{R}^{mN_C} \tag{B11}$$

and

$$V_N(\Delta x_{k+1}, \Delta\bar{u}_{k+1}) = V_N^*(\Delta x_k) \underbrace{-\Delta x_k^T P \Delta x_k - \Delta\hat{u}_k^{*T} R \Delta\hat{u}_k^* - \Delta\hat{x}_{k+N}^{*T} P_f \Delta\hat{x}_{k+N}^*}_{\text{remove}} \tag{B12}$$
$$\underbrace{+\Delta\hat{x}_{k+N}^{*T} P \Delta\hat{x}_{k+N}^* + \Delta\hat{u}^T R_N \Delta\hat{u} + \left(A_d\Delta\hat{x}_{k+N}^* + B_d\Delta\hat{u}\right)^T P_f \left(A_d\Delta\hat{x}_{k+N}^* + B_d\Delta\hat{u}\right)}_{\text{add}}$$

with R_N as shown in (44). Figure B1 shows a graphical representation of that change in the cost.
If there exists $\Delta\hat{u} = \kappa_f(\Delta x_k)$ such that

$$(A_d\Delta x_k + B_d\Delta\hat{u})^T P_f (A_d\Delta x_k + B_d\Delta\hat{u}) - \Delta x_k P_f \Delta x_k + \Delta x_k^T P \Delta x_k + \Delta\hat{u}^T R_N \Delta\hat{u} \leq 0 \tag{B13}$$

is fulfilled, then the difference in the value functions for subsequent iterations can be written as

$$V_N^*(\Delta x_{k+1}) - V_N^*(\Delta x_k) \leq -\Delta x_k^T P \Delta x_k - \Delta\hat{u}_k^{*T} R \Delta\hat{u}_k^* \tag{B14}$$

$\forall\Delta x_k \in \mathbb{R}^n$ and $V_f = \Delta x_k^T P_f \Delta x_k$ is a global CLF. Because of constraints, relations (B13) and (B14) are only requested locally, ie, $\forall\Delta x_k \in \delta\mathbb{X}_f$. With a linear ansatz $\Delta\hat{u} = \kappa_f(\Delta x_k) = K\Delta x_k$ relation (B13) turns into (43), if

$$K = -\left(B_d^T P_f B_d + R_N\right)^{-1} B_d^T P_f A_d \tag{B15}$$

and $\delta\mathbb{X}_f$ is chosen as the maximal admissible set[30] for the infinite horizon problem (see the work of Mayne et al[5]).

Assumption 1(a) together with Proposition 1 ensure that in the inner control loop is observable in sliding, which starts at the very beginning. As a result, $\Delta u_k \to 0$, $\Delta y_k \to 0$ and $\Delta x_k \to 0$.[2] This means that the closed-loop system consisting of an OISM controller, an OISM observer, and the tracking MPC (see Figure 1) is exponentially stable with a region of attraction $\delta\mathbb{X}_N$ and $x \to x_S$ respectively $z \to z_S$ is achieved.